Biotribology 18 (2019) 100096

Contents lists available at ScienceDirect

Biotribology

journal homepage: www.elsevier.com/locate/biotri

Changes in the morphology of microgrooved stem tapers with differing assembly conditions

Karl Dransfield*, Radu Racasan, James Williamson, Paul Bills

EPSRC Future Advanced Metrology Hub, University of Huddersfield, Huddersfield HD1 3DH, United Kingdom

ARTICLE INFO

Keywords:
Stem taper
Taper measurement
Metal-on-metal
Taper engagement

ABSTRACT

Background: Fretting and corrosion at the head-stem taper junction has been cited as a potential clinical concern. Material loss measurement is a vital tool for quantifying changes due to in vitro, in vivo, and/or ex-vivo implant experience. Material loss measurement requires reconstruction of pre-implantation geometry to delineate damage. This is straightforward in principle for plain machined tapers, integrating between a fitted interpolated cone and the measured data. Mathematical filtration methods have been developed to remove this texture and facilitate measurement. The extent to which the assembly process could influence filtration accuracy is not currently known.

Methods: An engagement/ disengagement study was performed on 27 head/ stem pairs using 2, 4, and 8kN impact loads. Impact was delivered in three locations; axial, 10° anterior, and 10° anteroproximal. Pull-off force was measured, and stems were measured pre and post assembly using a Talyrond 365 roundness measurement machine.

Results: An increase in the plastic deformation of microgrooves and pull-off force was noted with increasing assembly loads. Off-axis impaction resulted in reduced pull-off strength and reduced uniform microgroove distortion. Volumetric change between pre and post assembly was below the noise threshold on stem and head surfaces.

Discussion: The measurement method was shown to be capable of capturing linear microgroove deformation of 1 μm peak – peak and volume loss above $0.1mm^3$. Lower peak load was noted when impacting a seated head when compared with engagement of discrete heads and stems, under the same assembly conditions.

1. Introduction

Head-stem modularity in hip arthroplasty was introduced in the 1970s [1], initially to improve the wear characteristics of bearing pairs by enabling the use of mixed-material articulations, in particular the use of ceramics [2,3]. A well optimised hip arthroplasty offers increased range of motion and reduced likelihood of dislocation compared to an implant not suited to a patient's intrinsic anatomy. With modular designs, reconstruction of a patient's specific anatomic function can be achieved through trial reduction without removal of the stem, reducing the requirement for large component inventory [2,4]. Despite the valuable benefits offered by head-stem modularity, wear and corrosion at the taper junction has been documented as a potential clinical concern [3,5–21]. Termed MACC (Mechanically Assisted Crevice Corrosion), the issue of trunnion fretting corrosion is multifaceted; numerous variables involving patients, surgeons, and implant design have been recognised in the literature as contributors. A recurring mechanism, MACC, has been described as a synergistic mechanical and galvanic process: the generation of a corrosive environment through cyclic microdisplacements at the junction disturbing the passivation layers and aqueous intrusion within the interface crevice [8,16,17]. Larger femoral head diameters have recently been a popular surgical trend to improve joint stability, however the increased frictional torque has been suggested to increase taper fretting [22]. Insufficient impact force during surgery has also been raised as a concern [1,23]. The outcomes of these mechanisms are the wear and corrosion of the metallic surfaces, releasing wear debris and corrosion products into surrounding tissue. The response of the body to these products has elicited complications for patients. Psuedotumours, ALTRs (Adverse Local Tissue Reactions), ALVAL (Aseptic Lymphocyte-dominated Vasculitis Associated Lesion), periprosthetic osteolysis, and pain are all problems which have been linked with high taper wear [5–7] and corrosion, requiring invasive revision surgery to remedy.

The research effort surrounding the topic of taper fretting corrosion

* Corresponding author.
E-mail address: karl.dransfield@hud.ac.uk (K. Dransfield).

https://doi.org/10.1016/j.biotri.2019.100096
Received 10 December 2018; Received in revised form 18 April 2019; Accepted 23 April 2019
Available online 25 April 2019

is widespread, and numerous approaches have been adopted to correlate the network of variables with in vivo function. The use of metrology tools is one such method which is key to quantifying and understanding the performance of a specific medical device. Wear measurement of retrieved components relies upon the presence of some as-manufactured data from which to reconstruct the pre-implantation taper geometry. It is the numerical comparison of the reconstruction and the retrieved state which can be used as a quantitative measure of implant performance.

Modern stem taper designs are commonly machined with periodic radial ridges, also termed microgrooves. Such surface texturing was initially incorporated into hip arthroplasty design to prevent shattering (burst fracture) of brittle natured ceramic femoral heads by reducing local hoop stress peaks [24]. A stem taper has been said to be 'microgrooved' if it possesses a periodic surface texture with an amplitude of > 4 µm, and a wavelength over 100 µm [25]. Retrieved microgrooved stem tapers introduce challenges in reconstructing pre-implantation data. Where a smooth taper would be reconstructed by performing linear interpolation between areas not exhibiting damage, it is not possible to use this approach on microgrooved stem tapers. An alternative approach is required whereby the microgroove texture of a user identified 'as manufactured' area is mathematically modelled and evaluated over the remaining taper length, producing a reconstruction of the pre-implantation geometry [26,27].

The design intent is that microgrooves collapse during assembly, and the compressive stress exerted by the smooth head taper bore on the groove peaks sets up a state of interference [28]. Despite the exploitation of this design rationale in most modern modular designs, there is no standardisation of groove topography, varying not only between manufacturers, but also between product ranges of the same manufacturer [29]. Furthermore, medical device manufacturers seldom offer standardised recommendations on the surgical technique used to assemble stem and head pairs.

Previous studies have investigated the effect of assembly conditions on taper contact mechanics [1,24,29–33]. An increase in assembly force has been implicated with an improvement in taper interlock, reduction in fretting corrosion [29], and an increase in microgroove deformation [24]. Throughout the literature, 4 kN is regarded as a standard assembly force, with 2 kN and 8 kN encapsulating the upper and lower boundaries respectively [1,29,31,34]. It is feasible that these force ranges could be seen clinically based on differences in surgical technique. Positioning of the impactor relative to the pole of the head is entirely reliant on surgical skill. The effects of off-axis impaction have been investigated [30] in bi-modular hip arthroplasty. The location of impact was found to significantly influence the magnitude of force transmission to the taper junction. The effects of off-axis impaction have not yet been investigated for designs with head-stem modularity alone.

Pull off force has been used as an indicator of taper performance [30,32,33,35,36] and an active ASTM test method is available to assess the axial locking force of modular tapers [37]. Previous methods of assessing taper interlock strength have included metrological assessment of stem taper microgroove deformation before and after assembly. This has been undertaken previously with profilometry techniques [24], which recognised that ridge deformation and therefore taper contact area increases with assembly force. A recent publication [29] made use of a Talyrond 365 out-of-roundness measurement machine to measure a baseline stem taper volume as manufactured, and claimed to have performed volumetric wear analysis following cyclic loading, however did not present the results from this.

As surgical technique lacks standardisation, it is unknown how the lack of control over assembly conditions could influence the integrity of the perceived as-manufactured data from which microgroove extrapolation is performed when analysing wear. To understand how surgical technique could affect plastic microgroove deformation, measurement of the taper surfaces before and after assembly would be required.

The aim of this study was to develop a validated measurement and analysis procedure for quantification of plastic microgroove deformation, caused by seating and removal of the femoral head. A cohort of 27 stem and head pairs were assembled (varying impact magnitude and location), before being dis-engaged and re-measured, to benchmark the method and investigate how this process could affect the perceived material loss. This is an important consideration for the measurement of material loss from revised or wear simulated stem tapers.

2. Methodology

The proposed methodology would utilise metrology tools to visualise and quantify the changes in surface texture at the taper junction following assembly with three assembly forces delivered at three different impact locations. This entailed the following sequence: as-manufactured stem measurement, assembly, disassembly, and disassembled stem measurement. A single design of Ti-6Al-4 V stem with microgrooved surface texture and CoCrMo head were employed as a representative cohort of typical MoM designs.

2.1. Cohort

Components were assembled with three impact forces: 2, 4, and 8 kN, at three impact locations: Axial (on the pole of the head), 10° anterior of pole, and 10° anteroproximal of the pole (Fig. 1).

Each test was repeated three times, for any findings to hold statistical significance and be externally relevant. The experiment matrix in Table 1 summarizes assembly tests.

2.2. Measurement

The short wavelength roughness of the microgrooves rendered conventional stylus-based measurement techniques such as a coordinate measuring machine (CMM) unsuitable due to the high level of mechanical filtering associated with even small spherical styli. A measurement method with high lateral and vertical resolution was required to capture the asperities of the stem surface. To this end, all measurements in this study were performed using a roundness measurement machine: Talyrond 365 (Ametek Inc., US), which has been used in numerous previous studies to characterise both head and stem surfaces [19,29,38]. The Talyrond can capture straightness, roundness and cylindricity with sub-micron resolution, making use of an inductive transducer with a 1.2 nm resolution and 2 mm gauge range to identify height information. All components were first subjected to an iterative centring and levelling process to align the component with the spindle

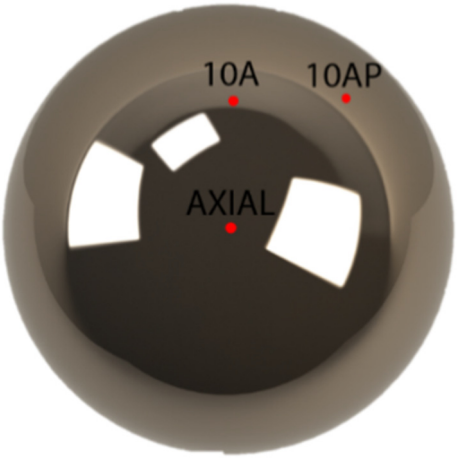

Fig. 1. Locations of impact delivery around femoral head.

Table 1
Experiment matrix showing impact magnitude and location.

Impact location	Impaction force		
	2 kN	4 kN	8 kN
Axial	$n = 3$	$n = 3$	n = 3
Anterior (10°)	n = 3	n = 3	n = 3
Anteroproximal (10°)	n = 3	n = 3	n = 3
Total components	27		

axis.

Stems were coupled to the Talyrond spindle via a compound angle goniometer stage to permit longitudinal and lateral alignment of the stem relative to the measurement co-ordinate system. Once each component was manually positioned on the rotational stage with minimal runout and angle mismatch, plane separated roundness traces were taken from the stem surface until an eccentricity of under 1 µm and angular deviation of $< 0.01^{\circ}$ was established between the axis of the turntable and that of the component. For centring and levelling of the textured stems, the mechanical filtering effects of a 2 mm spherical ruby stylus were exploited to suppress the influence of the rough texture on the alignment outcome.

Stem tapers were measured using the 'cylinder map' function, which collected a prescribed number of vertical straightness traces orthogonal to the surface texture, equally spaced around the taper circumference. Measurement routines were carried out with a 5 µm radius conisphere diamond stylus at a measurement speed of 1 mm/s. Sensitivity analysis deemed 180 vertical traces at 2° separation sufficient for data collection. Markings on the stem tapers were used to define the starting angle for each measurement.

Head tapers were also measured in a similar manner, in accordance with a previously published and validated measurement technique [38]. 180 vertical traces were taken at a measurement speed of 1 mm/s within the head taper to form a cylinder map. Measurement and centring & levelling routines were performed using a 5 µm diamond conisphere stylus.

2.3. Assembly

Impact force was delivered to the head and stem pairs using a bespoke drop tower impactor (Fig. 2), with a sled mass of 5 kg. The presence of an introducer was replicated by fitting a Delrin® impactor head to the sled. The combination of the high sled mass and Delrin® impactor head reduced the likelihood of rebound. The drop tower impactor was instrumented with a Kistler 9031A piezoelectric load cell. Load cell output was displayed on a Tektronix DPO 2014B oscilloscope following amplification by a Kistler 5073 charge amplifier. Calibration of the load washer involved placing a static mass on the impactor sled and equating the displayed voltage with the known force being exerted by the mass under gravity.

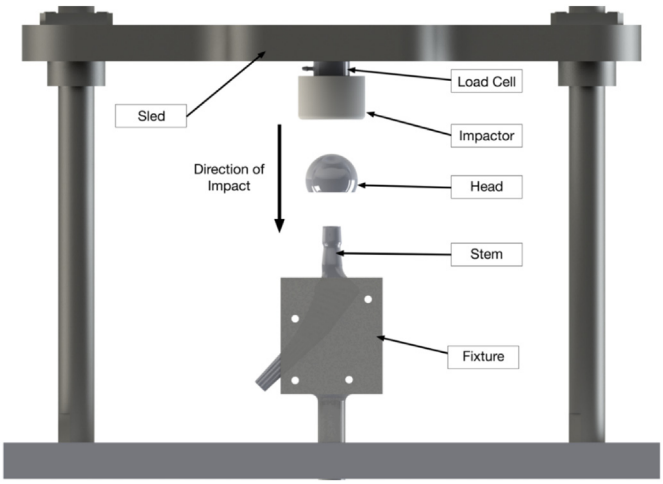

Fig. 2. Diagram of drop test rig apparatus.

It was necessary that each component was consistently and accurately oriented to reflect the desired assembly scenario, whilst also being held in a manner which ensured consistent levels of compliance between tests. Consequently, the chosen design of stem was scanned using Computed Tomography (CT) to construct a parametric 3D model, from which 3D printed fixtures were produced from Polylactic Acid (PLA) with 100% infill. Impact location was varied by using different 3D printed fixtures (Fig. 3), where the angle of the mounting spigot was adjusted in relation to the axis of the stem taper.

2.4. Distraction

Previous literature calibrated drop height on a seated head [1]. In this study, for reasons which will be covered hereafter, drop heights were calibrated on unassembled head/ stem pairs and load was measured for all tests.

Stems were distracted using an Instron (Instron Corporation, Norwood, MA, USA) 3369 tensile testing machine, in accordance with ASTM F2009–00. Fig. 4 shows the equipment configuration for the distraction study. A steady state axial tensile load was exerted on the underside of the femoral head, taking care to maintain a load axis angle within 1° of the longitudinal axis of the taper, by utilizing dedicated fixturing for the given stem design. Tensile load was applied at a constant displacement rate of 0.05 mm/s. Each test terminated when the applied distraction load reached 90% of the peak distraction load, indicating that the stem and head tapers were no longer engaged.

2.5. Analysis

Data analysis was carried out using an array of bespoke tools developed in MATLAB R2017b (The MathWorks, Inc., Natick, USA). Talyrond profile data was stitched to form a rectangular areal map and imported into MATLAB as a 2.5D matrix. Both pre and post assembly data sets were imported to allow simultaneous comparison.

A previously documented and validated method for form removal from taper surfaces was used to remove elliptical and conical form [38]. The study aim was to characterise pre and post-assembly changes to groove morphology, meaning only roughness information was of interest. This was achieved by tracewise polynomial fitting, where a second order polynomial curve was fitted to each trace from the cylinder map and the error from the fitted curve evaluated. Fig. 5 demonstrates the effect of form removal on a stem taper measurement.

Measurement start points were established manually, so it was unavoidable that each start point would not be identical. The result of this was axial misalignment of the pre and post assembly surfaces. Misalignment was quantified by searching for the scalar axial deviation between the two data sets which returned the highest Pearson correlation coefficient, then subsequently corrected (Fig. 6) using circular shifting between the pre and post assembly data sets (an operation which rearranges entries from the start of an array to the end). The limitation of this method was that a small amount of data, below one microgroove wavelength (200 µm), was rendered invalid due to the circular shifting.

Data alignment permitted generation of a residual map, which demonstrated the changes to surface texture, sustained during assembly. This was created by calculating the pairwise distance between data sets. This method provided a useful quantitative demonstration of damage distribution. Texture deformation was quantified by comparing average amplitude before and after assembly. Contact points were identified using a rolling ball morphological filter (Fig. 7). As the valleys of the texture should have experienced no permanent deformation from

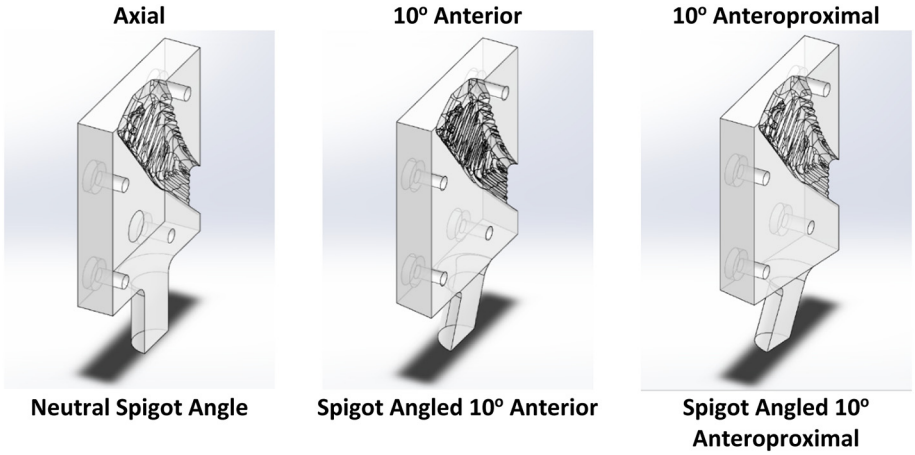

Fig. 3. CAD models showing one of two halves of fixtures used for engagement and disengagement.

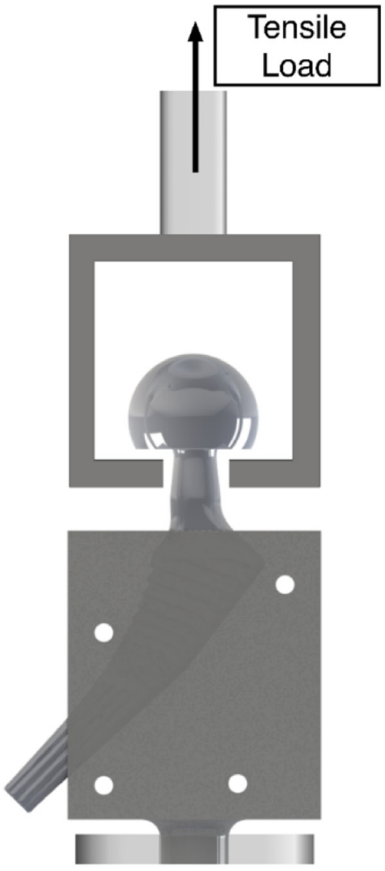

Fig. 4. Configuration of pull-off apparatus.

engagement and disengagement, the valley closing profiles were used as a vertical alignment datum between data sets.

The material displacement volume refers to the volume of micro-groove texture affected by the assembly process. This metric is demonstrated by the shaded region of a stem taper profile traced in Fig. 8. Material displacement volume was evaluated by performing trapezoidal numerical integration on both the pre and post assembly surfaces; the difference between these two volumes equated to the material displacement volume. Since volume was conserved regardless of the circular array shifting, quantification of the magnitude of material affected by the assembly process was possible.

An Abbott-Firestone curve [39] representing the cumulative probability density of the surface heights was generated for both pre and post-assembly data sets. Data was thresholded such that only data residing above the zero plane was included in the volume calculations to minimise the effect of any outliers present in the bottom of the groove topography. This is demonstrated by Fig. 9 below.

Head tapers were analysed using a previously developed and validated set of software tools [38]. Data sets underwent a multi-stage form removal process. Firstly, conical form was removed using a linear least squares fit. If present, secondary quadratic form, referred to as "barrelling" or "hogging", caused by the manufacturing process, could be removed with a further first or second order polynomial fit. Volume calculation was performed on the form removed data set by fitting a plane and integrating between the plane and the measured data. Thresholding was not required for the non-implanted heads being analysed in this study, as this is typically only used for removal of iatrogenic damage and surface debris from retrieval measurements.

2.6. Method validation & repeatability analysis

A study was carried out to assess the validity and repeatability of the measurement and analysis methodologies. A single as-manufactured stem of the same manufacturer and design as used in the main cohort was selected to conduct the repeatability study. The previously outlined measurement and analysis methodology was iterated 11 times in total; a baseline measurement and 10 further comparison measurements. Each component was removed from the measurement instrument, and the centring and levelling routine repeated between measurements.

The method of impact delivery was validated by repeating 10 impact tests on a seated head from a constant drop height. The analysis procedure was performed by a single operator and compared with the baseline measurement for volume and linear compression to determine the noise level. These tests factored in a $2.26 \times 10^{-6}\,mm^3$ floating point error generated by MATLAB, slight differences in positioning when measuring the stem caused by manual angular alignment with 0^o and location of the trace start point, equipment resolution, and any slight residual waviness following form removal.

The volume measurement was validated on mathematically generated surface data. Two surfaces were created, each with a 10-period square waveform (Fig. 10) allowing straightforward hand calculation of a known enclosed volume. The grid size of this data equated to that of a 12/14 taper with a length of 10 mm. Surface one was assigned a peak-peak amplitude of 20 µm, and surface two an amplitude of 10 µm, to simulate the presence of assembly damage. Both surfaces were simultaneously passed through the previously detailed algorithm and the output compared with the hand calculation result. The theoretical enclosed volume was calculated as follows:

$$Vol = Vol_{pre} - Vol_{post}$$

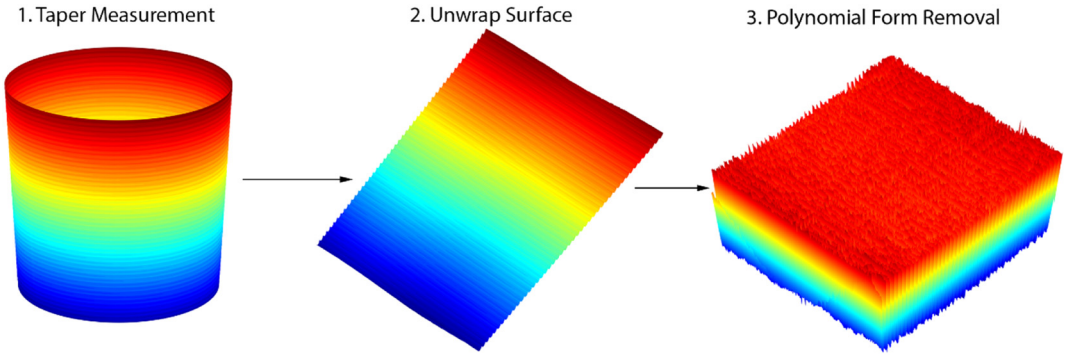

Fig. 5. Surface height maps showing form removal effects.

where:

$$Vol_{pre} = \frac{Length \times Circumference \times Amplitude}{2}$$

3. Results

3.1. Validation

The theoretical volume change for the simulated surfaces was found to be 2.042 mm^3. The volume change calculated by the algorithm was 2.0449 mm^3; a deviation of 0.0029 mm^3. This result verified the suitability of the volume calculation algorithm for calculation of the material displacement volume.

3.2. Repeatability analysis

Measured impact loads showed a high degree of repeatability ($\sigma = 0.05$). Results of measurement repeatability are presented in Table 2. Volume and average amplitude differences when measuring the same component were assessed to establish a baseline noise level and a minimum value for measurable change. Results for volume showed a sensitive and highly repeatable methodology with a noise level of ~0.01 mm^3 ($\sigma = 0.0055$).

Analysis showed that changes in average amplitude < 0.1 μm could be detected by the developed methodology, albeit at a larger standard deviation for volumetric changes ($\sigma = 0.295$). It is likely that the increased inter-measurement variation for the detection of amplitude-based changes, when compared with volumetric changes, is caused by the method being reliant upon detection and averaging of morphological extremes from profile traces with sporadic outliers.

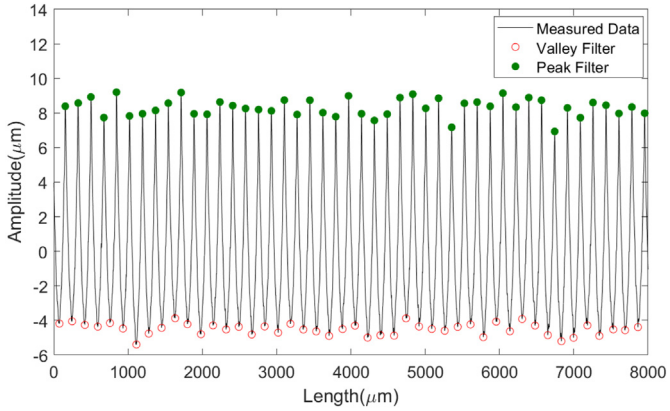

Fig. 7. Stem taper profile trace - discovering local minima and maxima with morphological closing filter.

3.3. Visualisation

Comparison of surface plots from corresponding pre and post assembly data sets revealed visible changes in topography as a result of the assembly process. Visual inspection revealed observable compression of the groove texture. Small amounts of concave form error (shown by arrows in Fig. 11) present on some stem tapers appeared to be compensated for, with the stem topography conforming to that of the head taper.

Residual maps were found to be of value in visualising the distribution of assembly damage around the circumference and length of the taper simultaneously. Positive values indicate compression of the groove texture. Fig. 12 shows the effect of assembly using axial load.

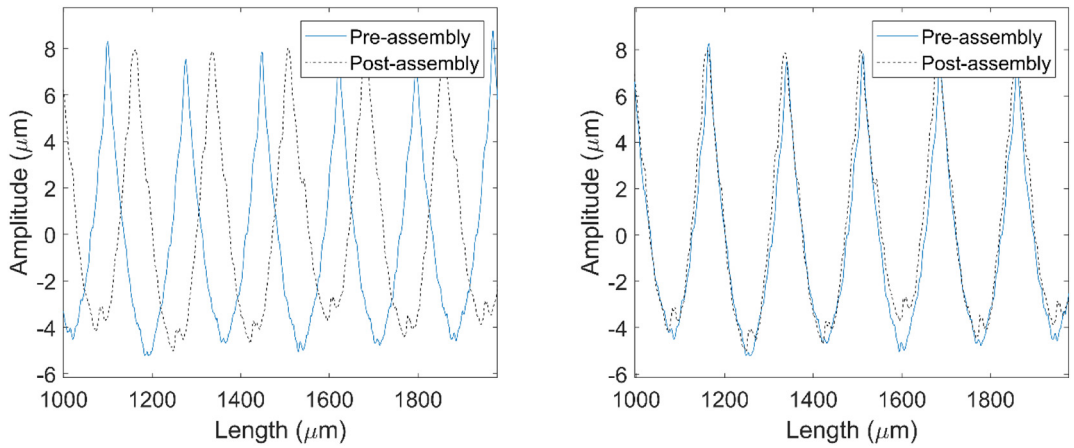

Fig. 6. Stem taper profiles before axial alignment procedure (Left) and after axial alignment procedure (Right).

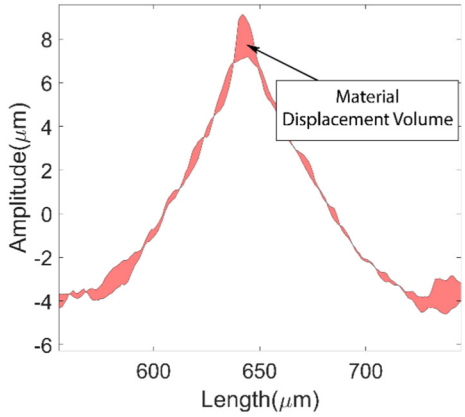

Fig. 8. Profile Trace of Stem Taper Pre and Post Assembly - Area Shaded Red Indicates Volume Affected by Assembly. (For interpretation of the references to colour in this figure legend, the reader is referred to the web version of this article.)

A progressive increase in global peak deformation was observed with increasing impact load. When varying impact location, a progressive decrease in global peak deformation was observed as impact moved away from the pole of the femoral head. Fig. 13 shows residual plots for 8kN impact loads delivered at all three locations. On these plots, an angle of 270° corresponds with the direction of the 10° anterior load, and an angle of 315° with the direction of application of the 10° anteroproximal load. Compression of the groove texture was not found to be directionally dependant, with no apparent increase in localised damage at the angles corresponding to the direction of force delivery, over the surrounding uniform distortion.

3.4. Physical observations

3.4.1. Assembly

Fig. 14 demonstrates the range of forces applied to the femoral heads in all the studied assembly scenarios. This was an important finding, as the assumption that the desired impact loads were being achieved based on the drop height calibration of seated head and stem pairs would have skewed subsequent findings.

3.4.2. Impulse

Previously published literature has measured impulse to compare the effects of varying impactor material [1]. Impulse values for a 4 kN peak force were between 2.99 Ns and 3.95 Ns, for rubber and polymeric impactor materials. Impulse and peak impact load in these assembly scenarios were not perfectly concurrent (Fig. 15).

3.4.3. Disassembly

Peak disassembly forces were recorded for all distraction events. The 8 kN anteroproximal case recorded the highest peak disassembly force, although it is worth noting that these samples were assembled with the highest median impact load and impulse of the 8 kN cohort. Pull-off force alone, as has been the standard of quantifying taper performance in several publications to date, is only a valid metric if assembly force has been tightly controlled. As the assembly data showed, this is challenging to achieve (Fig. 16).

3.4.4. Interlock efficiency ratio

To compensate for the variations in applied peak impact load across the cohorts, the interlock efficiency ratio was used. This was calculated by dividing the peak pull-off force (kN) by the peak impact load (kN). In all cases, an axial delivery resulted in a higher median pull-off strength for each newton of applied impact load. The application of impact load 10° anterior of the head pole resulted in a stronger interlock over the 10° anteroproximal delivery in the 2 kN case, whereas the converse was true in the 4 kN and 8 kN cases (Fig. 17).

3.5. Metrology results

3.5.1. Head taper volume

The noise level present in the measurement of head taper volume for the method used is in the region of 0.7 mm^3. This is due to the volume occupied by the machining texture of the taper surface. A cut-off of over 1 mm^3 was therefore defined for any volumetric changes to be valid. No head tapers measured in this study showed any signs of damage or measurable volumetric change.

3.5.2. Stem tapers - material displacement volume

A minimum measurable material displacement volume was dictated by the results of the repeatability analysis. Material displacement volume values below 0.1 mm^3 were deemed unfeasible to detect due to the noise level between repeat measurements being up to ~0.02 mm^3. For all measurements, differences in volume were below the measurable threshold of 0.1 mm^3.

3.5.3. Stem tapers - global compression

Global compression of the microgroove morphology was characterised by the average reduction in overall texture amplitude caused by the process of engagement and disengagement. An increase in the amount of texture compression was noted with increasing impact load, which agrees with previous findings [1] and the design philosophy of adding microgrooves to stem tapers.

4. Discussion

A new approach for characterising the changes in texture morphology of microgrooved stem tapers following assembly was presented in this study. Application of metrology tools provided access to areal data with which to compare stem tapers pre and post assembly. It was visually perceptible by comparing surface maps pre and post assembly, especially in the case of the higher loads, that the taper surfaces had

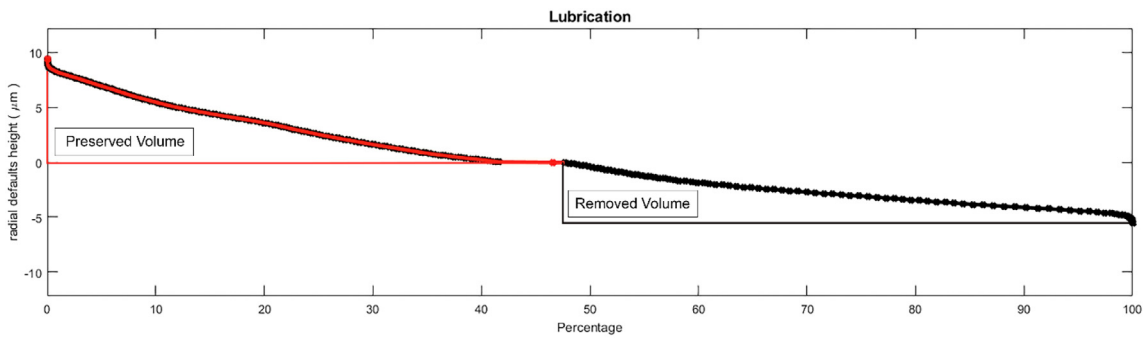

Fig. 9. Thresholding of stem taper data sets to zero plane to facilitate measurement of material displacement volume.

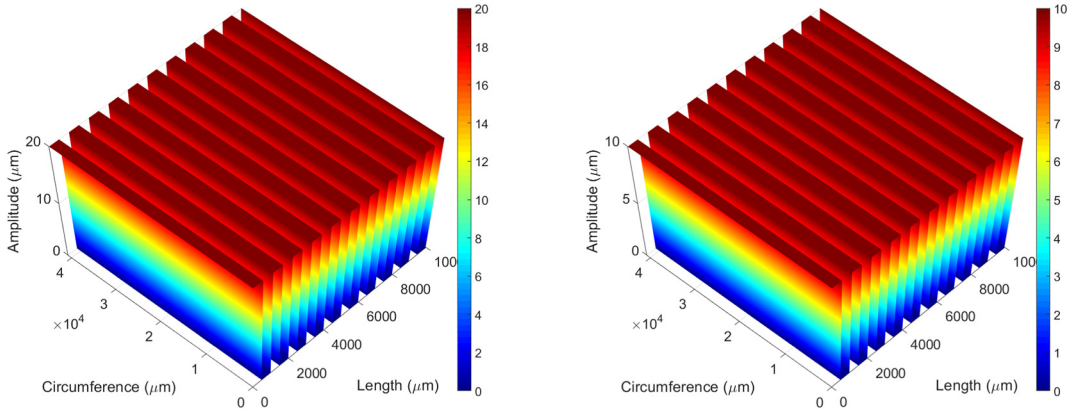

Fig. 10. Simulated surface data with 20 μm amplitude (left) and 10 μm amplitude (Right).

Table 2
Results from Repeatibility Analysis for Material Displacement Volume and Mean Global Texture Compression.

	Volume (mm^3)	Mean Global Compression (μm)
Mean	0.0099	0.0489
Median	0.0109	0.0623
Range	0.0023–0.0185	0.0039–0.0933
Standard Deviation	0.0055	0.295

sustained deformation. In some cases, stems possessed a slight concave form. This form was removed following assembly, as microgrooves conformed more at the distal and proximal extremities. A surface map of linear deviation between the pre and post assembly cases was created to delineate these changes more clearly. A noise level of 1 μm peak – peak was established for these surface maps by comparing repeat measurements of the same component. Generally, an increase in global plastic microgroove deformation was observed with increasing peak load.

Previously documented work made use of piezoelectric load cells to calibrate assembly equipment [1]. The same approach was followed at the beginning of this work – the drop tower impactor sled was released from differing heights until three heights were established which achieved the desired impact loads, based on impaction of a head-stem pair which were already assembled. When impacting the assembled head-stem pair, impact load remained consistent and predictable based on the prescribed drop heights. When using these drop heights to assemble components, however, the impact load delivered to the femoral head decreased, and despite the sled being released from a constant height, the forces achieved were not consistent or predictable. This was immediately apparent from the variation in impact load shown in Fig. 14. The fixturing used for the testing remained constant between all tests – inter-implant variation was the only change between tests. According to the work-energy principle, an increase in the distance travelled after an impact reduces the peak force experienced by the object being impacted. The reduction in force could therefore be attributed to the added interface compliance between the head and stem taper, with the seating of the taper during assembly reducing the force by increasing the deformation distance of the impact.

Pull-off force as a taper performance indicator has been utilised in most publications surrounding the topic of hip taper assembly thus far. This study concurred with the consensus that an increase in the amount of assembly force results in a stronger taper interlock between the femoral head and femoral stem. Pull-off force alone was not found to be a useful metric for assessing taper performance under given assembly scenarios - an 8kN impact delivered 10° anteroproximal of the pole resulted in the most secure connection, however these tests also received the highest assembly loads. To compensate for deviations from the targeted assembly loads, the interlock efficiency ratio was calculated. This metric indicated how well each taper connection performed in pull-off tests whilst accounting for each unit of impact load delivered in assembly. In concurrence with previous findings on bi-modular hip arthroplasty [30], it was observed that an axial impact performed the best in all cases and off-axis impaction reduced interlock efficiency. Whilst the 2kN axial force was found to yield the most efficient interlock, the interlock efficiency ratio is not an indicator of absolute taper strength. The findings of this study do not therefore contradict the consensus within the orthopaedic community that greater assembly

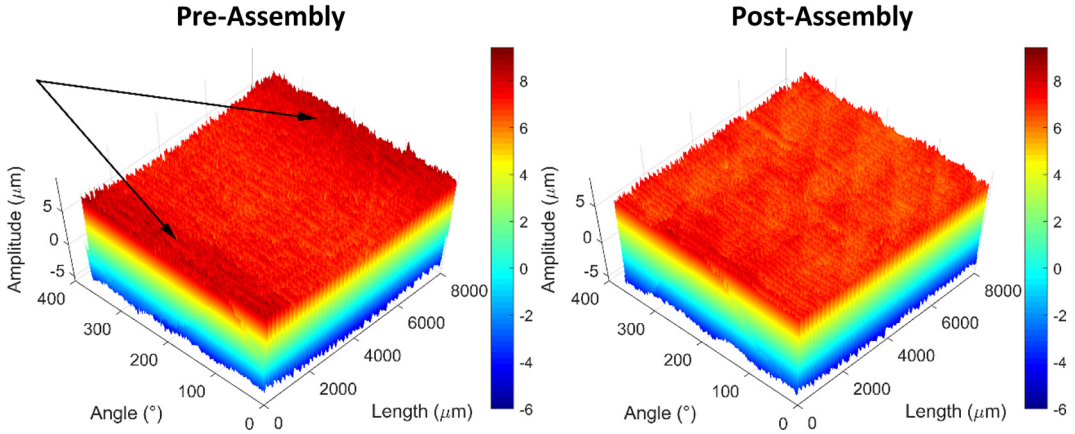

Fig. 11. Pre and Post Assembly Surface Maps Showing Flattening (Right) of Slightly Concave Surface (Left). Arrows Indicate Raised Areas at Distal and Proximal Extremities.

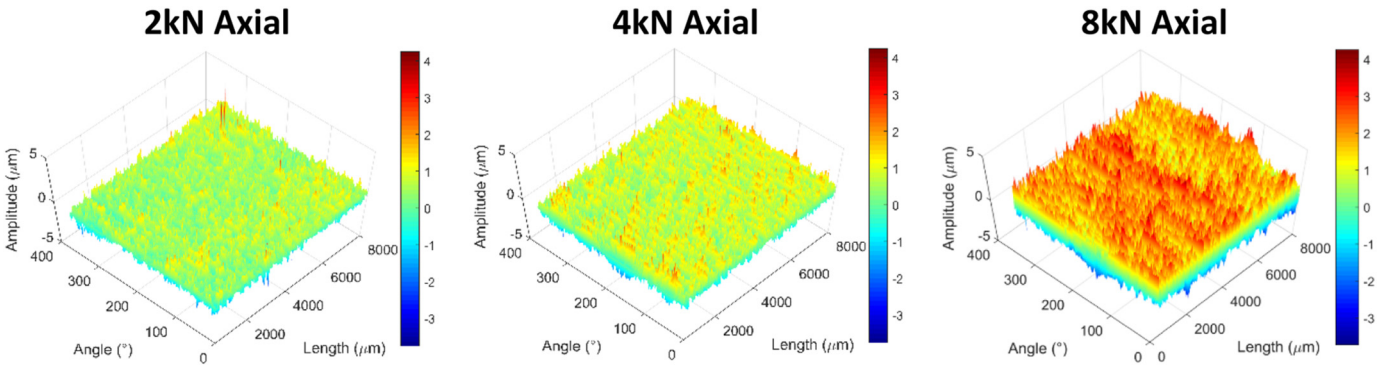

Fig. 12. Residual plots demonstrating the magnitude and distribution of texture distortion following assembly with increasing impact load.

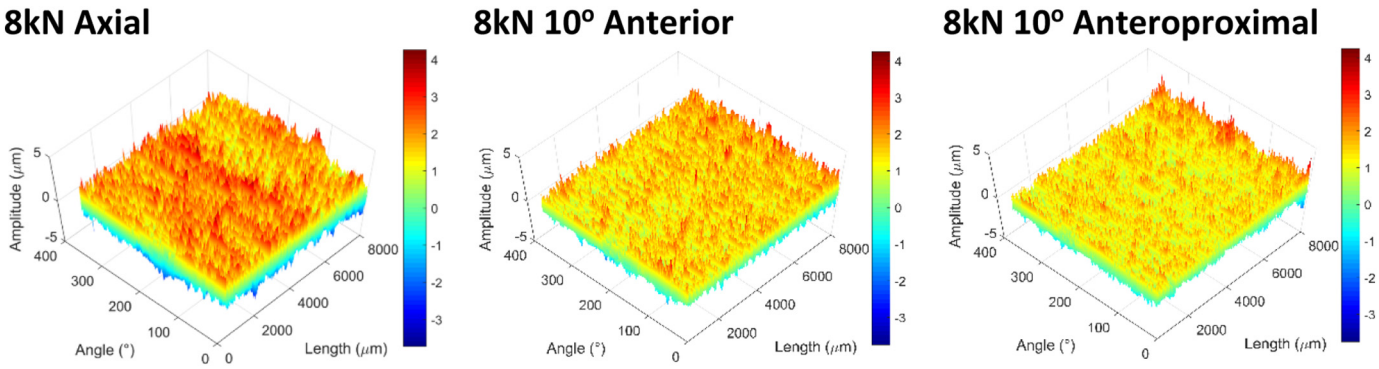

Fig. 13. Residual plots demonstrating the magnitude and distribution of texture distortion following assembly with impact load delivered at three locations.

loads are conducive to stronger taper interlock.

The 20 kHz sampling rate used for impact measurement resulted in a large amount of information from each impact event. It was noted that when performing impaction on pre-assembled head-stem pairs, a smooth, well defined impact spike was generated, reaching the desired peak load before decaying. When delivering impact load to assemble head-stem pairs, an oscillatory impulse spike was obtained, exhibiting between two to four peaks of increasing amplitude up to the intended peak force (Fig. 18).

This was observed in all assembly tests and could potentially be a phenomenon of taper seating. The combination of a high drop rig sled mass (5 kg), short impulse event (~4 ms), and that this was not occurring on pre-assembled pairs, suggests this is not a consequence of a second or further strike due to impactor rebound.

Despite the detectable increase in compression of the stem taper microgrooves with increasing impact load, the measured volume occupied by the material being compressed was extremely small. This was caused by the steep and narrow microgroove texture specific to this implant design – the base of the compressed microgroove peak was ~6 μm wide. When measuring retrieved components, the potential error caused by assembly and disassembly of the head and stem is therefore not only a function of how much the microgroove texture is deforming, but also implant-specific texture shape.

When off-axis impaction was performed, no directionality to the texture distortion was observed. At 10°, the impaction angles were not extreme, so it is not currently known if directional distortion and non-uniform taper fixation could occur as impaction drifts further from the pole of the femoral head.

Limitations were identified during this experiment. Firstly, as previously mentioned, assembly force is difficult to control when using

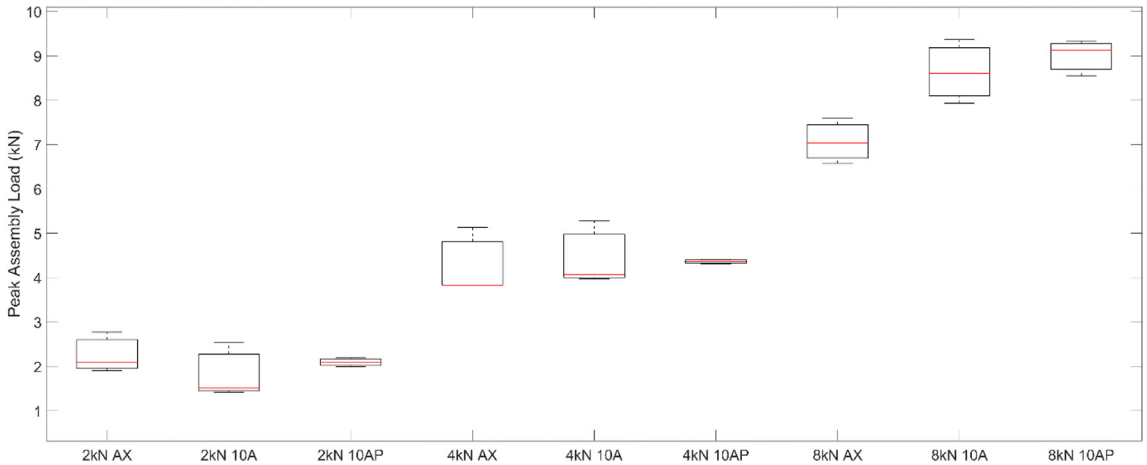

Fig. 14. Plot of peak assembly load delivered to the femoral head for all assembly scenarios.

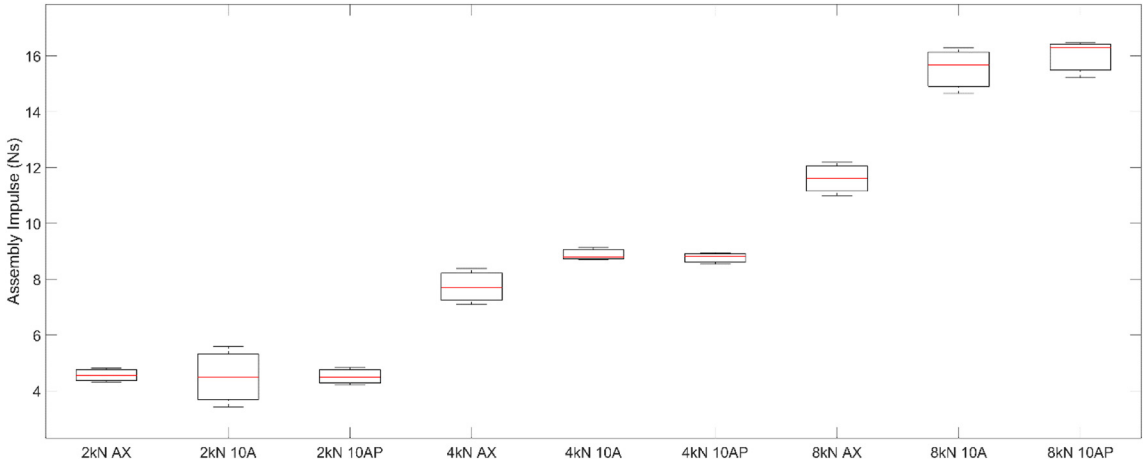

Fig. 15. Plot of applied impulse for all assembly scenarios.

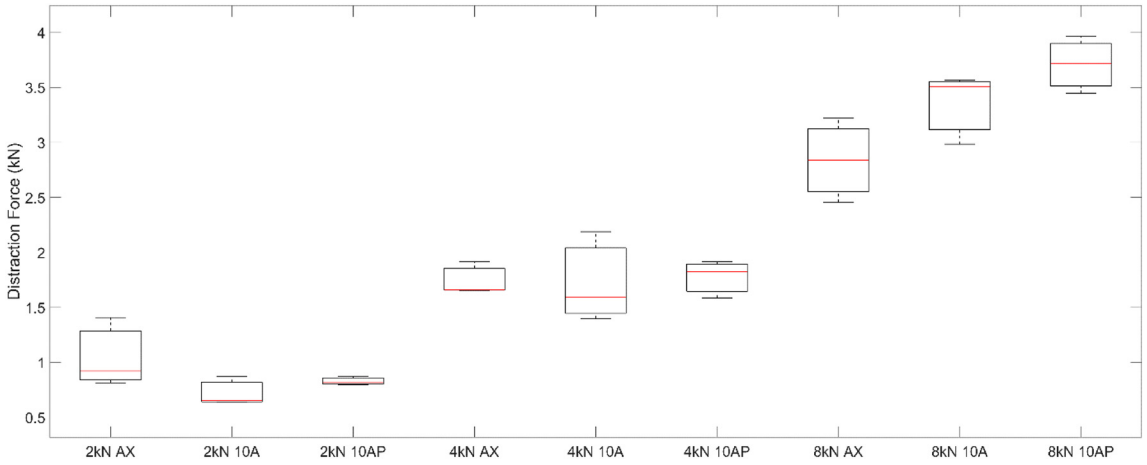

Fig. 16. Plot demonstrating variation in pull-off force based on differing assembly conditions.

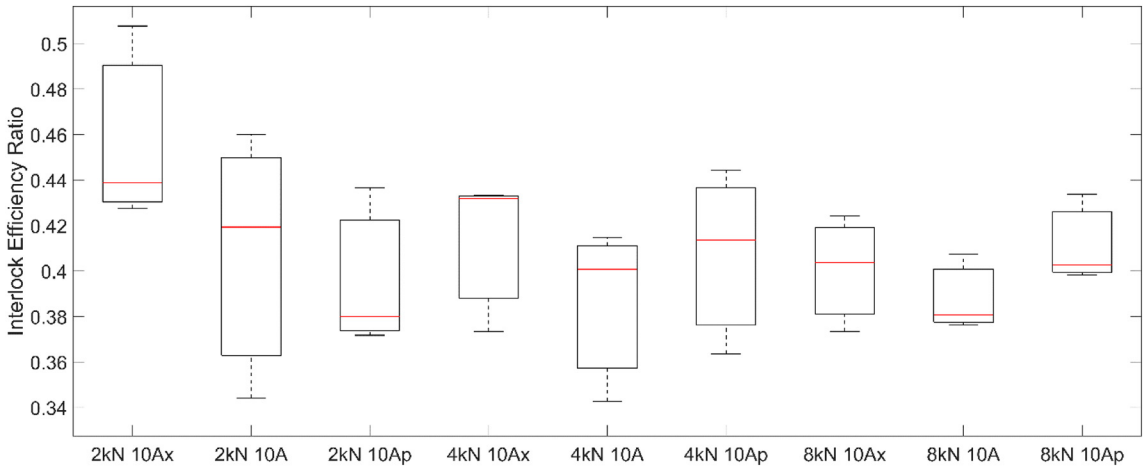

Fig. 17. Interlock efficiency ratio for varying assembly forces and delivery locations.

impact delivery with no means of closed loop feedback to monitor the force being delivered. This resulted in a variety of impact forces being applied, rather than the targeted 2, 4, and 8 kN assembly loads. Despite this, the method of impact delivery used in this study was comparable to surgical assembly. Damage quantification relied on accurate alignment of pre and post-assembly measurements. Without integrating the measurement and testing instrumentation, it was not feasible to perfectly re-align components manually, resulting in non-direct comparison of trace data. The effect of this was some in residual maps and error calculating global distortion. This limitation of the experimental set-up dictated an accuracy limit for the measurement of linear and volumetric damage, which was quantified by repeatability analysis.

5. Conclusions

This study has shown that modern metrology tools can be used to

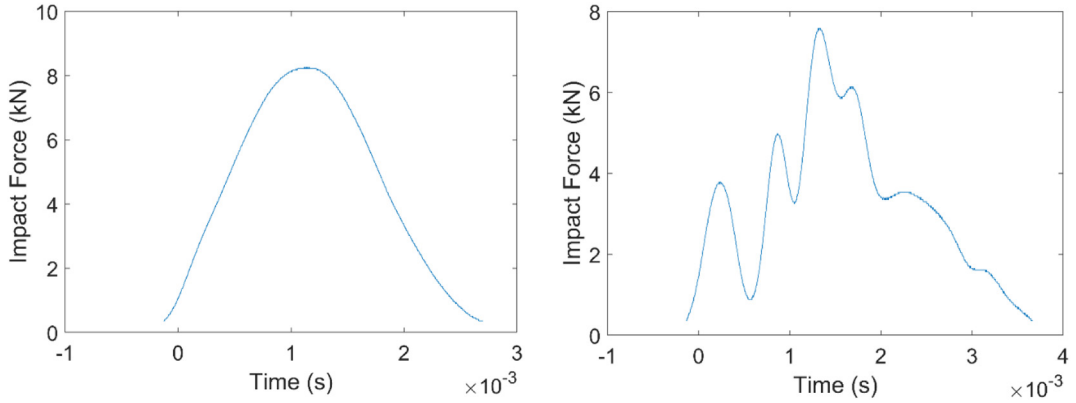

Fig. 18. Impulse response for a pre-assembled head/stem pair (Left) and for assembling a head/stem pair (Right).

characterise changes at the taper junction sustained due to assembly processes. The microgroove texture was observed to follow the intended design philosophy, with the peaks collapsing during assembly. This study demonstrated that force and directionality of impact applied by surgeons hold the potential to influence this process, with higher loads increasing the amount of texture deformation and resulting in a stronger taper interlock. As impact load was delivered further from the pole of the femoral head, a reduction in deformation and pull-off force was observed. Form mismatch was found to be compensated for by the harder alloy femoral head – slightly concave stems were flattened, whilst any damage to the head taper was not detectable. The perceived volume lost from the peaks of the microgroove texture was seen to be dependent on a combination of surgical load and the manufacturer specific surface morphology. Narrower microgroove topography elicited a reduction in perceived volume loss for the same amount of linear microgroove displacement.

Conflict of interest statement

The authors whose names are listed immediately below report the following details of affiliation or involvement in an organization or entity with a financial or non-financial interest in the subject matter or materials discussed in this manuscript.

Author names:

- Mr. Karl Dransfield
- Dr. Radu Racasan
- Dr. James Williamson
- Dr. Paul Bills

The authors gratefully acknowledge the UK's Engineering and Physical Sciences Research Council (EPSRC) funding of the EPSRC Future Advanced Metrology Hub (Grant Ref: EP/P006930/1).

Financial and material support was appreciatively received from DePuy Synthes in the form of medical device supply, without which this study could not have been undertaken.

References

[1] A. Rehmer, N.E. Bishop, M.M. Morlock, Influence of assembly procedure and material combination on the strength of the taper connection at the head-neck junction of modular hip endoprostheses, Clin. Biomech. (Bristol, Avon) 27 (1) (2012) 77–83.
[2] H.U. Cameron, Modularity in primary total hip arthroplasty, J. Arthroplast. 11 (3) (1996) 332–334.
[3] J.P. Collier, V.A. Surprenant, R.E. Jensen, M.B. Mayor, H.P. Surprenant, Corrosion between the components of modular femoral hip prostheses, J. Bone Joint Surg. Br. Vol. 74 (4) (1992) 511–517.
[4] W.J. Hozack, J.J. Mesa, R.H. Rothman, Head-neck modularity for total hip arthroplasty. Is it necessary? J. Arthroplast. 11 (4) (1996) 397–399.
[5] R. Chana, C. Esposito, P.A. Campbell, W.K. Walter, W.L. Walter, Mixing and matching causing taper wear: corrosion associated with pseudotumour formation, J. Bone Joint Surg. Br. Vol. 94 (2) (2012) 281–286.
[6] M.J. Chmell, D. Rispler, R. Poss, The impact of modularity in total hip arthroplasty, Clin. Orthop. Relat. Res. (319) (1995) 77-84.
[7] R.B. Cook, B.J. Bolland, J.A. Wharton, S. Tilley, J.M. Latham, R.J. Wood, Pseudotumour formation due to tribocorrosion at the taper interface of large diameter metal on polymer modular total hip replacements, J. Arthroplast. 28 (8) (2013) 1430–1436.
[8] H.J. Cooper, C.J. Della Valle, J.J. Jacobs, Biologic implications of taper corrosion in total hip arthroplasty, Semin. Arthroplast. 23 (4) (2012) 273–278.
[9] R.M. Dyrkacz, J.M. Brandt, O.A. Ojo, T.R. Turgeon, U.P. Wyss, The influence of head size on corrosion and fretting behaviour at the head-neck interface of artificial hip joints, J. Arthroplast. 28 (6) (2013) 1036–1040.
[10] K.B. Fricka, H. Ho, W.J. Peace, C.A. Engh, Metal-on-metal local tissue reaction is associated with corrosion of the head taper junction J. Arthroplast. 27(8, Supplement) (2012) 26–31.e1.
[11] J. Gilbert, J.J. Jacobs, The Mechanical and Electrochemical Processes Associated with Taper Fretting Crevice Corrosion: A Review, (1997).
[12] J.L. Gilbert, C.A. Buckley, J.J. Jacobs, In vivo corrosion of modular hip prosthesis components in mixed and similar metal combinations. The effect of crevice, stress, motion, and alloy coupling, J. Biomed. Mater. Res. 27 (12) (1993) 1533–1544.
[13] I.P.S. Gill, J. Webb, K. Sloan, R.J. Beaver, Corrosion at the neck-stem junction as a cause of metal ion release and pseudotumour formation, J. Bone Joint Surg. Br. Vol. 94-B (7) (2012) 895–900.
[14] G. Grammatopoulos, H. Pandit, D.W. Murray, H.S. Gill, The relationship between head-neck ratio and pseudotumour formation in metal-on-metal resurfacing arthroplasty of the hip, J. Bone Joint Surg. Br. Vol. 92 (11) (2010) 1527–1534.
[15] J. Hart Alister, K. Matthies Ashley, J. Bills Paul, R. Radu, B. Gordon, B. Liam, S. John, The Taper Junction Contributes One Third of the Total Volumetric Material Loss in Large Diameter Metal-on-Metal Hip Arthroplasties, American Academy of Orthopaedic Surgeons Annual Meeting, Chicago, IL, USA, 2013.
[16] J.J. Jacobs, J.L. Gilbert, R.M. Urban, Corrosion of metal orthopaedic implants, J. Bone Joint Surg. Am. 80 (2) (1998) 268–282.
[17] J.J. Jacobs, R.M. Urban, J.L. Gilbert, A.K. Skipor, J. Black, M. Jasty, J.O. Galante, Local and distant products from modularity, Clin. Orthop. Relat. Res. (319) (1995) 94-105.
[18] A. Matthies, R. Underwood, P. Cann, K. Ilo, Z. Nawaz, J. Skinner, A.J. Hart, Retrieval analysis of 240 metal-on-metal hip components, comparing modular total hip replacement with hip resurfacing, J. Bone Joint Surg. Br. Vol. 93 (3) (2011) 307–314.
[19] K. Matthies Ashley, R. Racasan, P. Bills, L. Blunt, S. Cro, A. Panagiotidou, G. Blunn, J. Skinner, J. Hart Alister, Material loss at the taper junction of retrieved large head metal-on-metal total hip replacements, J. Orthop. Res. 31 (11) (2013) 1677–1685.
[20] A. Patel, J. Bliss, R.P. Calfee, J. Froehlich, R. Limbird, Modular femoral stem-sleeve junction failure after primary total hip arthroplasty, J. Arthroplast. 24 (7) (2009) (1143.e1-5).
[21] J.G. Skendzel, J.D. Blaha, A.G. Urquhart, Total hip arthroplasty modular neck failure, J. Arthroplast. 26 (2) (2011) (338.e1–4).
[22] J.M. Elkins, J.J. Callaghan, T.D. Brown, Stability and trunnion wear potential in large-diameter metal-on-metal total hips: a finite element analysis, Clin. Orthop. Relat. Res. 472 (2) (2014) 529–542.
[23] P.J. Bills, R. Racasan, P. Tessier, L.A. Blunt, Assessing the material loss of the modular taper interface in retrieved metal-on-metal hip replacements, Surf. Topogr. Metrol. Prop. 3 (2) (2015).
[24] F. Witt, J. Gührs, M.M. Morlock, N.E. Bishop, Quantification of the contact area at the head-stem taper Interface of modular hip prostheses, PLoS One 10 (8) (2015) e0135517.
[25] C.M. Arnholt, D.W. MacDonald, R.J. Underwood, E.P. Guyer, C.M. Rimnac, S.M. Kurtz, C. Implant Research Center Writing, M.A. Mont, G.R. Klein, G.-C. Lee, A.F. Chen, B.R. Hamlin, H.E. Cates, A.L. Malkani, M.J. Kraay, Do stem taper microgrooves influence taper corrosion in Total hip arthroplasty? A matched cohort retrieval study, J. Arthroplast. 32 (4) (2017) 1363–1373.
[26] K. Dransfield, R. Racasan, L. Blunt, P. Bills, Characterization of Material Loss from Femoral Stem Taper Surfaces through Development of a Responsive Morphological

Filtering Technique, (2018), pp. 173–190.
[27] S.B. Kocagoz, R.J. Underwood, D.W. MacDonald, J.L. Gilbert, S.M. Kurtz, Ceramic heads decrease metal release caused by head-taper fretting and corrosion, Clin. Orthop. Relat. Res. 474 (4) (2016) 985–994.
[28] S. Hussenbocus, D. Kosuge, L.B. Solomon, D.W. Howie, R.H. Oskouei, Head-neck taper corrosion in hip arthroplasty, Biomed. Res. Int. (2015) (2015) 758123.
[29] A. Panagiotidou, T. Cobb, J. Meswania, J. Skinner, A. Hart, F. Haddad, G. Blunn, Effect of impact assembly on the interface deformation and fretting corrosion of modular hip tapers: an in vitro study, J. Orthop. Res. 36 (1) (2018) 405–416.
[30] N.B. Frisch, J.R. Lynch, R.F. Banglmaier, C.D. Silverton, The effect of impact location on force transmission to the modular junctions of dual-taper modular hip implants, J. Arthroplast. 31 (9) (2016) 2053–2057.
[31] M.L. Mroczkowski, J.S. Hertzler, S.M. Humphrey, T. Johnson, C.R. Blanchard, Effect of impact assembly on the fretting corrosion of modular hip tapers, J. Orthop. Res. 24 (2) (2006) 271–279.
[32] A.T. Pennock, A.H. Schmidt, C.A. Bourgeault, Morse-type tapers: factors that may influence taper strength during total hip arthroplasty, J. Arthroplast. 17 (6) (2002) 773–778.
[33] A.H. Schmidt, D.A. Loch, J.E. Bechtold, R.F. Kyle, Assessing Morse taper function: The relationship between impaction force, disassembly force, and design variables, Modularity of Orthopedic Implants, ASTM International, 1997.
[34] J.P. Heiney, S. Battula, G.A. Vrabec, A. Parikh, R. Blice, A.J. Schoenfeld, G.O. Njus, Impact magnitudes applied by surgeons and their importance when applying the femoral head onto the Morse taper for total hip arthroplasty, Arch. Orthop. Trauma Surg. 129 (6) (2009) 793–796.
[35] S. Jauch, A. Miles, H. Gill, Does the surface finish, the taper angle difference and the assembly force effect the taper strength between stem and ball head of a modular hip implant? Orthopaedic Research Society 2014 Annual Meeting, University of Bath, 2014.
[36] C.J. Lavernia, L. Baerga, R.L. Barrack, E. Tozakoglou, S.D. Cook, L. Lata, M.D. Rossi, The effects of blood and fat on Morse taper disassembly forces, Am. J. Orthop. 38 (4) (2009) 187–190 (Belle Mead, N.J.).
[37] Standard ASTM, Test Method for Determining the Axial Disassembly Force of Taper Connections of Modular Prostheses, West Conshohocken, PA (2011).
[38] R. Racasan, P.J. Bills, L. Blunt, A. Hart, J. Skinner, Method for Characterization of Material Loss from Modular Head-Stem Taper Surfaces of Hip Replacement Devices, Modularity and Tapers in Total Joint Replacement Devices, ASTM International, West Conschohocken, PA, 2015, pp. 132–146.
[39] E.J. Abbott, F.A. Firestone, Specifying surface quality - a method on accurate measurement and comparison, Mech. Eng. ASME 55 (1933) 569–572.